Received: 7 January 2022 | Revised: 4 March 2023 | Accepted: 9 March 2023

DOI: 10.1002/mma.9254

RESEARCH ARTICLE

WILEY

Mathematical modeling of pest resistance to insecticides in a heterogeneous environment

Kada Khadidja Aicha[2] | **Ainseba Bedreddine**[1] | **Bouguima Sidi Mohammed**[2]

[1]Bordeaux University, IMB UMR CNRS 5251, Talence, France

[2]Department of Mathematics, labo: Systémes Dynamiques et applications, University of Tlemcen, Tlemcen, Algeria

Correspondence
Ainseba Bedreddine, Bordeaux University, IMB UMR CNRS 5251, Talence, France.
Email: bedreddine.ainseba@u-bordeaux.fr

Communicated by: E. Venturino

Insecticides are an effective tool for controlling grapevine moths such as *Lobesia botrana*. However, when massive use of insecticides, pests develop resistance because of selection of resistant individuals of the population and/or because of natural mutation. The main question is then to define a strategic pest management with respect to time and space. In the first part of this work, we present a model without spatial structure describing the dynamics of insects including its resistance to insecticides. In the second part, we include in the model dispersal between different space patches. Individuals can move from one patch to another at a fast time scale with respect to the demographical time scale. Using this model, we aim to understand the main characteristics leading to persistence or extinction of the insect pest population. We establish global stability results. Numerical simulations provide some interesting insights on the dynamics of the pest population.

KEYWORDS

aggregated model, basic offspring number, cooperative systems, insects, juveniles and adults, slow fast dynamics

MSC CLASSIFICATION

37N25, 37C65, 92B05

1 | INTRODUCTION

The European grapevine moth *Lobesia botrana* causes major economic damages in many European countries (France, Italy, etc.), North Africa, and in many Asian countries [1, 2]. This pest requires constant control. The means of control used by winegrowers can be summed up in three approaches: biological control with sexual and food traps, chemicals with insecticides, and mathematical modeling for the prediction and the treatment effectiveness. The ability to disperse is a life trait of the pest. In the present study, the space is modeled by several patches (see Levins [3]). Pesticides have been extensively used to control the insect pest population at its first generations and at its different stages: eggs, larvae, pupae, and adults; see, for instance, Irigaray et al. [4]. As a massive use of insecticides, insects develops resistance. This is what ecologists call natural selection of the resistant individuals. But this can also happen when areas are treated with insecticides with little effect [5]. Due to the difficulties of experimentally assessing the impact of an insecticide on insect resistance, mathematical models are an important tool for studying sustainable pest control. Recently, analytical models for grapevine moth population dynamics have been developed providing strategic control of the insect; see Ainseba et al. [6] and Picart and Milner [7]. Spatial models with diffusion, where space is considered as a continuous variable is investigated in He [8]. However, none of these works have included insecticide resistance.

In this paper, a simple mathematical model that includes the above features is analyzed to understand the impact of insect resistance and movement on the dynamics of the insect pest population. We assume that the insect population is distributed in discrete patches. Thiéry et al. [9] study, using experimental data, the impact of intraspecific competition during the larvae stage on the development and adult fitness of the species. Similarly to Thiéry et al. [9], we show in this paper that the larvae crowding do not alter the reproduction capacity of the pest.

In the following sections, we develop and analyze a system of differential equations describing the population dynamics including three features of pest behavior that are relevant to *L. botrana*, namely, (a) insecticide resistance, (b) dispersal ability, and (c) larval competitiveness. We consider a mode of action that targets only adult insects.

We derive two mathematical models. The first one is analyzed without dispersal. For this model, we establish in Section 2 global stability of the equilibriums in terms of an index R_0. In Section 3, we develop a more complex model with dispersal. Individuals can move from one patch to another at a fast time scale with respect to the demographical time scale. After reduction of the model using aggregation methods, we establish global asymptotic behavior.

2 | THE IMMATURE–MATURE MODEL WITH INSECTICIDE RESISTANCE

Depending on climatic conditions, a female lay a mean of 35 eggs a day. Eggs remain until natural death or emerge into larvae. After a few days, the larvae develop into pupae that mature and emerge into adults.

In this work, for simplicity, we divide the insect population into two stages: the immature stage that includes all the preadult stages, that is, egg, larvae, and pupae and the adult one that corresponds to the reproductive stage. We assume that once an adult emerges, it is exposed to insecticides. For simplicity, we assume that larval stage is not affected by the type of insecticides we consider in this work.

Let's denote by $L(t)$ the density of individuals in the immature stage, by $V(t)$ the density of adults that are vulnerable to insecticides, and by $R(t)$ the density of resistant adults. From the description above, we obtain the following system of differential equations:

$$\begin{cases} \frac{dL}{dt} = \lambda_1 V + \lambda_2 R - rL - \mu_L L - cL^2, \\ \frac{dV}{dt} = \rho(rL) - \mu_V V - \delta V, \\ \frac{dR}{dt} = (1-\rho) rL - \mu_R R. \end{cases} \tag{1}$$

With initial conditions: $L(0) > 0$, $V(0) > 0$, $R(0) > 0$. The description of the parameters appearing in (1) is given in Table 1. All the parameters are measured per 1 day.

Larvae rarely leave the plant on which they were oviposited, this induces intraspecific competition during the larval stage; hence, the term $-cL$ represents a growth limit due to resource sharing. The exposition to insecticides may not in reality be permanent. The rate of mortality by insecticides is a function $\delta(t)$ varying with time. As an approximation, it is supposed that exposure to insecticides is constant with a rate δ representing the average of $\delta(t)$ over a life cycle. The level of resistance varies from one individual to another, but it is assumed to be negligible compared to natural mortality. In this model, we do not include fitness cost of resistance. Biologically, it is reasonable to assume that the growth rates, mortality rates of vulnerables and resistant insects are the same, but we analyze a more general mathematical model.

TABLE 1 Parameters of system (1) (see Picart [10]).

Parameters	Description	Values
δ	Insect mortality induced by insecticides	Unknown
λ_1	Birth rate of vulnerable	$[0.02, 0.8]$
λ_2	Birth rate of resistant	$[0.02, 0.8]$
r	Rate at which juvenils develop into adult	$[0.01, 0.8]$
c	Juvenile competition rate	Unknown
μ_L	Juvenile mortality rate	$[0.1, 0.85]$
μ_V	Vulnerable mortality rate	$[0.1, 0.87]$
μ_R	Resistant mortality rate	$[0.1, 0.87]$
$1-\rho$	Proportion of new resistant insect	$[0, 1]$

2.1 | Global existence and persistence

In the following, we denote by $\mathbb{R}_+^3 = \left\{(L, V, R) \in \mathbb{R}^3 : L \geqslant 0, V \geqslant 0, R \geqslant 0\right\}$. Let a,b $\in \mathbb{R}^3$.

Definition 1. We write

$$a \leq b,$$

if

$$b - a \in \mathbb{R}_+^3.$$

We write

$$a < b,$$

if

$$b - a \in \mathbb{R}_+^3 \backslash \{0\}.$$

We write

$$a << b,$$

if

$$b - a \in Int\left(\mathbb{R}_+^3\right).$$

The n-dimensional interval is defined by

$$[a, b] = \left\{x \in \mathbb{R}^3 : a \leq x \leq b\right\}.$$

Let $D \subset \mathbb{R}^3$ be an open domain. Consider the system of ODE's

$$\begin{cases} x'(t) = f(x(t)), \ x \in D, t > 0, \\ x(t_0) = x_0. \end{cases} \tag{2}$$

If $f : D \to \mathbb{R}^3$ is differentiable on a convex D, then the system (2) is said to be cooperative if the Jacobian matrix $\frac{df}{dx}$ is a Metzler matrix, for $x \in D$, and $t \geq 0$, that is, its off-diagonal entries are nonnegative. The system (2) is irreducible if the Jacobian matrix $\frac{df}{dx}$ is irreducible, that is, the corresponding graph is strongly connected; see Meyer [11].

Theorem 1.

(a) For all $X_0 = (L(0), V(0), R(0)) \in \mathbb{R}_+^3$, system (1) has a unique solution $(L(t), V(t), R(t)) \in \mathbb{R}_+^3$ for all $t \geqslant 0$.
(b) If $0 \leq \rho < 1$, then the solution $(L(t), V(t), R(t)) >> 0$, for all $t \geqslant 0$.

Proof.

(a) The right side of system (1) is C^1, then the solution exists and it is unique on a maximal interval $[0, T_{max}[$, with $T_{max} > 0$.

Consider the right side of the system

$$f(L, V, R) = \begin{pmatrix} \lambda_1 V + \lambda_2 R - rL - \mu_L L - cL^2, \\ \rho rL - \mu_V V - \delta V, \\ (1-\rho) rL - \mu_R R, \end{pmatrix}.$$

In $\mathbb{R}_+^3$, we see for system (1) that if $L = 0$, then $\frac{dL}{dt} \geq 0$, similarly if $V = 0$, then $\frac{dV}{dt} \geq 0$; and if $R = 0$, then $\frac{dR}{dt} \geq 0$. Therefore, $\mathbb{R}_+^3$ is positively invariant, which means that any trajectory of the system starting from an initial state in $\mathbb{R}^3_+$ remains in $\mathbb{R}^3_+$. The solution is positive on $[0, T_{max}[$. Now, we will show that the solution is globally defined. Let

$$P = L + V + R.$$

Then,

$$\begin{aligned}\frac{dP}{dt} &\leqslant \lambda_1 V + \lambda_2 R + rL \\ &\leqslant MP,\end{aligned}$$

where $M = max(\lambda_1, \lambda_2, r) > 0$. It follows that the solution is globally defined.

(b) Note that the Jacobian matrix of the system is given by

$$J(L, V, R) = \begin{pmatrix} -r - \mu_L - 2cL & \lambda_1 & \lambda_2 \\ \rho r & -\mu_V - \delta & 0 \\ (1-\rho)r & 0 & -\mu_R \end{pmatrix}.$$

We notice that elements outside the diagonal are all positive. Thus, system (1) is cooperative.

The Jacobian matrix is irreducible, that is, the corresponding graph is strongly connected, then the solution $(L(t), V(t), R(t)) >> 0$, for all $t \geqslant 0$.

□

2.2 | Local analysis of the model

The equilibrium points of system (1) satisfies

$$V^* = \frac{\rho r L^*}{\mu_V + \delta}, \tag{3}$$

and

$$R^* = \frac{(1-\rho) r L^*}{\mu_R}, \tag{4}$$

where L^* verifies that

$$\lambda_1 V^* + \lambda_2 R^* - rL^* - \mu_L L^* - cL^{*2} = 0. \tag{5}$$

A simple computation gives that

$$L^* = 0 \text{ or } L^* = \frac{1}{c}\left\{\frac{\lambda_1 \rho r}{\mu_V + \delta} + \frac{\lambda_2(1-\rho)r}{\mu_R} - (r + \mu_L)\right\}.$$

Thus, we have the extinction equilibrium and the nontrivial one, given by

$$\left(\frac{1}{c}\left\{\frac{\lambda_1 \rho r}{\mu_V + \delta} + \frac{\lambda_2(1-\rho)r}{\mu_R} - (r + \mu_L)\right\}, \frac{\rho r \frac{1}{c}\left\{\frac{\lambda_1 \rho r}{\mu_V + \delta} + \frac{\lambda_2(1-\rho)r}{\mu_R} - (r + \mu_L)\right\}}{\mu_V + \delta}, \frac{(1-\rho) r \frac{1}{c}\left\{\frac{\lambda_1 \rho r}{\mu_V + \delta} + \frac{\lambda_2(1-\rho)r}{\mu_R} - (r + \mu_L)\right\}}{\mu_R}\right).$$

Proposition 1. *The model (1) has exactly one equilibrium point in $\partial\mathbb{R}^3_+$ given by $P_0 = (0, 0, 0)$.*

2.3 | The basic offspring number

In order to compute the basic offspring number, we use the next generation technique; see van den Driessche and Watmough [12]. First, we write the system in the form

$$\frac{d}{dt}\begin{pmatrix} L \\ V \\ R \end{pmatrix} = F_1(L,V,R) + F_2(L,V,R),$$

$$F_1(L,V,R) = \begin{pmatrix} \lambda_1 V + \lambda_2 R \\ 0 \\ 0 \end{pmatrix},$$

and

$$F_2(L,V,R) = \begin{pmatrix} -rL - \mu_L L - cL^2 \\ \rho r L - \mu_V V - \delta V \\ (1-\rho) r L - \mu_R R \end{pmatrix}.$$

Then, direct computations of the Jacobians at $(L,V,R) = (0,0,0)$ give

$$-J_{F_1} J_{F_2}^{-1} = \begin{pmatrix} \frac{\lambda_1 \rho r}{(r+\mu_L)(\mu_V+\delta)} + \frac{\lambda_2(1-\rho)r}{\mu_R(r+\mu_L)} & \frac{\lambda_1}{\mu_V+\delta} & \frac{\lambda_2}{\mu_R} \\ 0 & 0 & 0 \\ 0 & 0 & 0 \end{pmatrix}.$$

Since the basic offspring reproduction number R_0 is by definition the spectral radius of $-J_{F_1} J_{F_2}^{-1}$, then

$$R_0 = \frac{\lambda_1 \rho r}{(r+\mu_L)(\mu_V+\delta)} + \frac{\lambda_2(1-\rho)r}{\mu_R(r+\mu_L)}.$$

Here,

$$\frac{1}{\mu_V+\delta} \text{ and } \frac{1}{\mu_R}$$

are, respectively, the average time of survival of the vulnerable and resistant adults. Similarly,

$$\frac{1}{(r+\mu_L)}$$

is the average time of survival of juveniles. The quantity

$$\frac{\lambda_1 \rho r}{(\mu_V+\delta)}$$

is the vulnerable adult production rate of juveniles, and

$$\frac{\lambda_2(1-\rho)r}{\mu_R}$$

is the resistant adult production rate of juveniles. Hence, R_0 is the adult production rate of juveniles.

We can write the second equilibrium point in terms of R_0 in the following manner:

$$(L^*, V^*, R^*) = \left(\frac{r+\mu_L}{c}(R_0-1), \frac{\rho r(r+\mu_L)}{c(\mu_V+\delta)}(R_0-1), \frac{(1-\rho)r(r+\mu_L)}{\mu_R c}(R_0-1) \right).$$

It is clear that

Proposition 2. *System (1) admits an interior equilibrium if* $R_0 > 1$.

2.4 | Global stability of extinction and interior equilibria

In this section, we will study stability of each equilibrium point of our system (1).

Theorem 2.

(a) If $R_0 \leq 1$, then $(0,0,0)$ is globally asymptotically stable in R^3_+.
(b) If $R_0 > 1$, (L^*, V^*, R^*) is globally asymptotically stable in $R^3_+ \setminus \{(L, V, R) : L = 0\}$.

Proof.

(a) **Stability of the equilibrium point** $(0,0,0)$: Let us look for an interval $[a, b] \subset \mathbb{R}^3_+$ such that $f(a) \geqslant 0$ and $f(b) \leqslant 0$, $a, b \in \mathbb{R}^3_+$; see, for instance, Theorem 6 in Anguelov et al. [13].
Take $a = (0,0,0)$, then $f(0,0,0) = 0 \geqslant 0$.
Let L_m be a positive number large enough such that

$$L^m \geqslant \frac{1}{c}\left(\frac{\lambda_1 \rho r}{\mu_V + \delta} + \frac{\lambda_2(1-\rho)r}{\mu_R} - (r + \mu_L)\right).$$

Let V^m and R^m be two positive constants such that

$$V^m = \frac{(\rho r)L^m}{\mu_V + \delta},$$
$$R^m = \frac{(1-\rho)rL^m}{\mu_R},$$

and

$$b^m = (L^m, V^m, R^m),$$

then, it is clear that

$$f(b^m) \leq 0.$$

Since $(0,0,0)$ is a unique equilibrium in $[a, b^m]$ for $R_0 < 1$, then $(0,0,0)$ is globally asymptotically stable in $[a, b^m]$, and since b^m can be selected larger than any fixed $x \in \mathbb{R}^3_+$, it follows that $(0,0,0)$ is globally asymptotically stable in $\mathbb{R}^3_+$.

(b) **Stability of the equilibrium point** (L^*, V^*, R^*):
Let $\varepsilon > 0$ and $L^\varepsilon > 0$ be small enough such that

$$L^\varepsilon \leq \varepsilon,$$

and

$$cL^\varepsilon < \lambda_1 \frac{(\rho r)}{\mu_V + \delta} + \frac{\lambda_2(1-\rho)r}{\mu_R} - \mu_L - r.$$

Let V^ε and R^ε be two positive constants such that

$$V^\varepsilon = \frac{(\rho r)L^\varepsilon}{\mu_V + \delta},$$

and

$$R^\varepsilon = \frac{(1-\rho)rL^\varepsilon}{\mu_R},$$

then

$$a^\varepsilon = (L^\varepsilon, V^\varepsilon, R^\varepsilon)$$

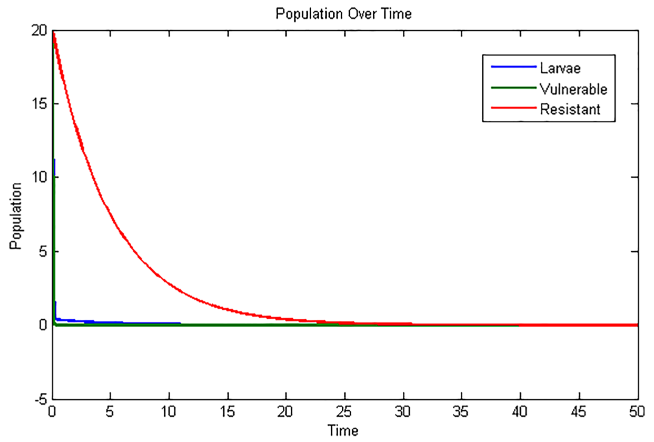

FIGURE 1 The behavior of system (1) trajectories for a reproduction rate $R_0 = 0.0096 < 1$. [Colour figure can be viewed at wileyonlinelibrary.com]

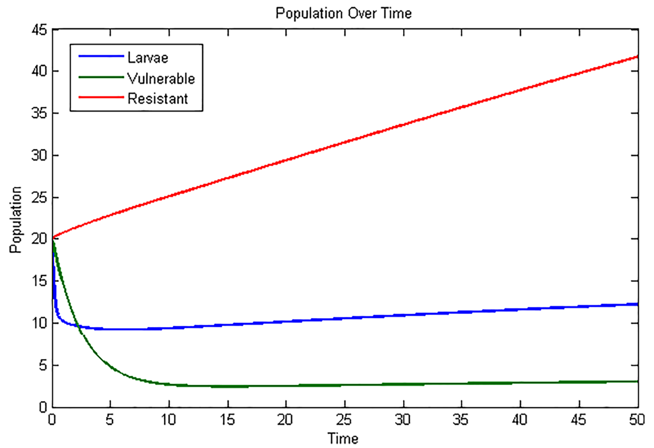

FIGURE 2 The behavior of system (1) trajectories for a reproduction rate $R_0 = 10.31 > 1$. [Colour figure can be viewed at wileyonlinelibrary.com]

TABLE 2 The values taken for the calculation of R_0 corresponding to Figure 2.

λ_1	λ_2	r	μ_L	c	μ_V	μ_R	ρ	δ
0.5	0.8	0.2	0.2	0.2	0.2	0.02	0.5	0.2

satisfies

$$f(a^\varepsilon) \geq 0.$$

When $R_0 > 1$, (L^*, V^*, R^*) is the unique equilibrium in $[a^\varepsilon, b^m]$. Since a^ε can be selected arbitraly small, and b^m larger than any $x > 0$, it follows that (L^*, V^*, R^*) is globally asymptotically stable in the interior of $\mathbb{R}^3_+$. Moreover, when $L = 0$, the equations of V and R are decreasing with respect to time and the solutions converge to zero. □

Corollary 1. *System (1) has a transcritical bifurcation around* $(0, 0, 0)$ *at* $R_0 = 1$.

2.5 | Numerical simulations

In this section, we give numerical simulations that confirm the analytical results. Figure 1 shows that the pest population is driven to extinction. In Figure 2, the parameter has been increased to $\lambda_2 = 0.8$ and the parameter μ_R is decreased to 0.02 with other parameters being the same as in Table 1, the figure shows persistence of the population. Due to insecticides, both figures show that resistant insects become dominant (Tables 2 and 3).

TABLE 3 The values taken for the calculation of R_0 corresponding to Figure 1.

λ_1	λ_2	r	μ_L	c	μ_V	μ_R	ρ	δ
0.5	0.4	0.2	20	0.2	0.2	0.2	0.5	40

3 | PATCHY ENVIRONMENT

In this section, we consider a more complex model, incorporating the movement of the insect. Let L_i, V_i, and R_i be respectively the larvae, vulnerable adult, and resistant adult densities in the patch i. In the sequel, we limit ourself to two patches. The model can be written as follows:

$$\begin{cases} \frac{dL_1}{dt} = \lambda_1 V_1 + \lambda_2 R_1 - r_1 L_1 - \mu_{L_1} L_1 - c_1 L_1^2, \\ \frac{dV_1}{dt} = \rho_1 (r_1 L_1) - \mu_{V_1} V_1 - \delta_1 V_1 - m^1 V_1 + m^2 V_2, \\ \frac{dR_1}{dt} = (1-\rho_1) r_1 L_1 - \mu_{R_1} R_1 - k^1 R_1 + k^2 R_2, \\ \frac{dL_2}{dt} = \beta_1 V_2 + \beta_2 R_2 - r_2 L_2 - \mu_{L_2} L_2 - c_2 L_2^2, \\ \frac{dV_2}{dt} = \rho_2 (r_2 L_2) - \mu_{V_2} V_2 - \delta_2 V_2 - m^2 V_2 + m^1 V_1, \\ \frac{dR_2}{dt} = (1-\rho_2) r_2 L_2 - \mu_{R_2} R_2 - k^2 R_2 + k^1 R_1, \end{cases} \tag{6}$$

where $m^i, i = 1, 2$ are, respectively, the rate of movement for vulnerable adults leaving patch i and $k^i, i = 1, 2$ are, respectively, the rate of movement of resistant adults leaving patch i. The other parameters keep the same definition as in the first model. For instance, β_1, and β_2 are, respectively, the birth rate of vulnerables and resistants in Patch 2. The parameters c_1, c_2 are, respectively, the juvenile competition rate in Patch 1 and Patch 2.

3.1 | Properties of system (6)

Proposition 3. *The set $\mathbb{R}_+^6$ is a positively invariant set for system (6).*

Proof. It is clear the $\mathbb{R}_+^6$ is forward positive. □

Proposition 4. *System (6) is cooperative.*

Proof. Simple computations show that the nondiagonal elements of the Jacobian matrix are positive; then, system (6) is cooperative. □

Proposition 5. *Suppose that the initial conditions belong to $\mathbb{R}_+^6$, then system (6) has a unique local solution that remains in $\mathbb{R}_+^6$ for all time, $t \geq 0$.*

Proof. Since the right side of system (6) is C^1, then system (6) has a unique local solution. The rest of the proposition is a direct consequence of proposition 3. □

Mathematical analysis of system (6) is difficult, so we will take advantage of the fact that the dynamical processes in model (6) evolve according to different time scales: a fast one for the movement between patches and a slow one, corresponding to the natural time, for the demography. Indeed the movement between the patches is of the order of the hour and the population growth is weekly and sometimes monthly. Under these considerations, system (6) can be written in the following form:

$$
\begin{cases}
\frac{dL_1}{dt} = \varepsilon(\lambda_1 V_1 + \lambda_2 R_1 - r_1 L_1 - \mu_{L_1} L_1 - c_1 L_1^2),\\
\frac{dV_1}{dt} = \varepsilon(\rho_1(r_1 L_1) - \mu_{V_1} V_1 - \delta_1 V_1) - m^1 V_1 + m^2 V_2,\\
\frac{dR_1}{dt} = \varepsilon((1-\rho_1) r_1 L_1 - \mu_{R_1} R_1) - k^1 R_1 + k^2 R_2,\\
\frac{dL_2}{dt} = \varepsilon(\beta_1 V_2 + \beta_2 R_2 - r_2 L_2 - \mu_{L_2} L_2 - c_2 L_2^2),\\
\frac{dV_2}{dt} = \varepsilon(\rho_2(r_2 L_2) - \mu_{V_2} V_2 - \delta_2 V_2) - m^2 V_2 + m^1 V_1,\\
\frac{dR_2}{dt} = \varepsilon((1-\rho_2) r_2 L_2 - \mu_{R_2} R_2) - k^2 R_2 + k^1 R_1,
\end{cases}
\tag{7}
$$

where ε is a small positive parameter which means that the reproductive process is very slow in comparison to the movement which has a larger speed. Here, t is the fast time.

In this case, it is possible to perform aggregation methods that allows to reduce the system (7) into a lower dimensional system; see Poggiale [14] and Auger and Bravo de la Parra [15] and the references therein. When ϵ is small enough, the reduced system approximates the asymptotic behavior of the initial system (7). Here, we consider the variables

$$
\begin{aligned}
R &:= R_1 + R_2,\\
V &:= V_1 + V_2.
\end{aligned}
$$

The system (7) can be considered as an ϵ-perturbation of the fast part obtained when $\epsilon = 0$. If $\epsilon = 0$, then

$$
\frac{dV}{dt} = \frac{dV_1}{dt} + \frac{dV_2}{dt} = 0,
$$

$$
\frac{dR}{dt} = \frac{dR_1}{dt} + \frac{dR_2}{dt} = 0.
$$

This means that V and R are first integrals for the fast part of system (7). The aggregation method consists in replacing the fast variables by their equilibrium values. To compute the fast equilibrium, we put $\varepsilon = 0$ in system (7). This gives that

$$
\begin{cases}
-m^1 V_1 + m^2 V_2 = 0,\\
-k^2 R_2 + k^1 R_1 = 0.
\end{cases}
\tag{8}
$$

Then,

$$
\begin{cases}
V_1^* = \frac{m^2}{m^1+m^2} V,\\
V_2^* = \frac{m^1}{m^1+m^2} V,\\
R_1^* = \frac{k^2}{k^1+k^2} R,\\
R_2^* = \frac{k^1}{k^1+k^2} R.
\end{cases}
\tag{9}
$$

The next step is to substitute the fast equilibrium in system (7). We obtain the following reduced system:

$$
\begin{cases}
\frac{dL_1}{d\tau} = \lambda_1 \frac{m^2}{m^1+m^2} V + \lambda_2 \frac{k^2}{k^1+k^2} R - r_1 L_1 - \mu_{L_1} L_1 - c_1 L_1^2,\\
\frac{dV}{d\tau} = \rho_1(r_1 L_1) + \rho_2(r_2 L_2) - \mu_{V_1} \frac{m^2}{m^1+m^2} V - \delta_1 \frac{m^2}{m^1+m^2} V - \mu_{V_2} \frac{m^1}{m^1+m^2} V - \delta_2 \frac{m^1}{m^1+m^2} V,\\
\frac{dR}{d\tau} = (1-\rho_1) r_1 L_1 + (1-\rho_2) r_2 L_2 - \mu_{R_1} \frac{k^2}{k^1+k^2} R - \mu_{R_2} \frac{k^1}{k^1+k^2} R,\\
\frac{dL_2}{d\tau} = \beta_1 \frac{m^1}{m^1+m^2} V + \beta_2 \frac{k^1}{k^1+k^2} R - r_2 L_2 - \mu_{L_2} L_2 - c_2 L_2^2,
\end{cases}
\tag{10}
$$

here,

$$\tau = \varepsilon t$$

is the slow time, and L_1, L_2, V, R are the slow variables.

Let

$$\frac{m^2}{m^1+m^2} = M_2 \quad \frac{k^2}{k^1+k^2} = K_2,$$
$$\frac{m^1}{m^1+m^2} = M_1 \quad \frac{k^1}{k^1+k^2} = K_1,$$

and

$$\mu_V = \mu_{V_1} M_2 + \mu_{V_2} M_1,$$
$$\mu_R = \mu_{R_1} K_2 + \mu_{R_2} K_1,$$
$$\delta = \delta_1 M_2 + \delta_2 M_1.$$

With the above assumptions, we formulate the reduced model as follows:

$$\begin{cases} \frac{dL_1}{d\tau} = \lambda_1 M_2 V + \lambda_2 K_2 R - r_1 L_1 - \mu_{L_1} L_1 - c_1 L_1^2, \\ \frac{dL_2}{d\tau} = \beta_1 M_1 V + \beta_2 K_1 R - r_2 L_2 - \mu_{L_2} L_2 - c_2 L_2^2, \\ \frac{dV}{d\tau} = \rho_1 r_1 L_1 + \rho_2 r_2 L_2 - \mu_V V - \delta V, \\ \frac{dR}{d\tau} = (1-\rho_1) r_1 L_1 + (1-\rho_2) r_2 L_2 - \mu_R R. \end{cases} \tag{11}$$

System (7) is composed of six equations while system (11) is composed of four equations. One can obtain the asymptotic behavior of (7) provided that more is known about the dynamics of (11); see Poggiale [14] and Harrak et al. [16].

3.2 | Analysis of the reduced model

We focus our attention on the model (11) which captures the main dynamic behavior of the population. We can easily notice that the trivial equilibrium $(0, 0, 0, 0)$ always exists for system (11).

3.2.1 | The basic offspring number

To derive the basic offspring number, we define

$$R_0^1 := \frac{\lambda_1 M_2 \rho_1 r_1}{(r_1 + \mu_{L_1})(\mu_V + \delta)} + \frac{\lambda_2 K_2 (1-\rho_1) r_1}{(r_1 + \mu_{L_1})\mu_R},$$
$$R_0^2 := \frac{\beta_1 M_1 \rho_2 r_2}{(r_2 + \mu_{L_2})(\mu_V + \delta)} + \frac{\beta_2 K_1 (1-\rho_2) r_2}{(r_2 + \mu_{L_2})\mu_R},$$
$$\alpha_2 := \frac{\lambda_1 M_2 \rho_2 r_2}{\mu_V + \delta} + \frac{\lambda_2 K_2 (1-\rho_2) r_2}{\mu_R},$$
$$\gamma_1 := \frac{\beta_1 M_1 \rho_1 r_1}{\mu_V + \delta} + \frac{\beta_2 K_1 (1-\rho_1) r_1}{\mu_R},$$

and

$$A := \frac{\alpha_2 \gamma_1}{(r_2 + \mu_{L_2})(r_1 + \mu_{L_1})}.$$

The linearized system of (11) at the trivial equilibrium is written in the form

$$\frac{dX}{dt} = (T + \Sigma)X,$$

with

$$T = \begin{pmatrix} 0 & 0 & \lambda_1 M_2 & \lambda_2 K_2 \\ 0 & 0 & \beta_1 M_1 & \beta_2 K_1 \\ 0 & 0 & 0 & 0 \\ 0 & 0 & 0 & 0 \end{pmatrix},$$

and

$$\Sigma = \begin{pmatrix} -(r_1 + \mu_{L_1}) & 0 & 0 & 0 \\ 0 & -(r_2 + \mu_{L_2}) & 0 & 0 \\ \rho_1 r_1 & \rho_2 r_2 & -(\mu_V + \delta) & 0 \\ (1-\rho_1) r_1 & (1-\rho_2) r_2 & 0 & -\mu_R \end{pmatrix}.$$

The basic offspring number is the spectral radius of the next generation matrix $K = -T\Sigma^{-1}$. Hence,

$$R_0 = \rho(K).$$

Simple calculations gives

$$\Sigma^{-1} = \begin{pmatrix} \frac{-1}{(r_1+\mu_{L_1})} & 0 & 0 & 0 \\ 0 & \frac{-1}{(r_2+\mu_{L_2})} & 0 & 0 \\ \frac{\rho_1 r_1}{(r_1+\mu_{L_1})(\mu_V+\delta)} & \frac{\rho_2 r_2}{(r_2+\mu_{L_2})(\mu_V+\delta)} & \frac{-1}{(\mu_V+\delta)} & 0 \\ \frac{(1-\rho_1) r_1}{(r_1+\mu_{L_1})(\mu_R)} & \frac{(1-\rho_2) r_2}{(r_2+\mu_{L_2})(\mu_R)} & 0 & \frac{-1}{\mu_R} \end{pmatrix},$$

and

$$K = \begin{pmatrix} R_0^1 & \frac{\alpha_2}{(r_2+\mu_{L_2})} & \frac{\lambda_1 M_2}{(\mu_V+\delta)} & \frac{\lambda_2 K_2}{\mu_R} \\ \frac{\gamma 1}{(r_1+\mu_{L_1})} & R_0^2 & \frac{\beta_2 M_1}{(\mu_V+\delta)} & \frac{\beta_2 K_2}{\mu_R} \\ 0 & 0 & 0 & 0 \\ 0 & 0 & 0 & 0 \end{pmatrix}.$$

With the concept of bloc matrices, we write

$$K = \begin{pmatrix} K_{11} & K_{12} \\ K_{21} & K_{22} \end{pmatrix},$$

with $K_{21} = K_{22}$ are the trivial matrices. The spectral radius of K is given by the large positive eigenvalue of the matrix

$$K_{11} = \begin{pmatrix} R_0^1 & \frac{\alpha_2}{(r_2+\mu_{L_2})} \\ \frac{\gamma 1}{(r_1+\mu_{L_1})} & R_0^2 \end{pmatrix}.$$

The characteristic equation is

$$\xi^2 - \left(R_0^1 + R_0^2\right)\xi + (R_0^1 R_0^2 - A) = 0.$$

Note that both eigenvalues are real since

$$\Delta = \left(R_0^1 + R_0^2\right)^2 - 4(R_0^1 R_0^2 - A) = \left(R_0^1 - R_0^2\right)^2 + 4A > 0.$$

Therefore, the basic offspring number is

$$R_0 = \frac{\left(R_0^1 + R_0^2\right) + \sqrt{\Delta}}{2}.$$

Note that the basic offspring number depends on the movement rate of adults. The biological interpretation of R_0 is not easy.

3.2.2 | Existence of an interior equilibrium point

From the third equation of system (11), we have

$$V = \frac{1}{\mu_V + \delta}(\rho_1 r_1 L_1 + \rho_2 r_2 L_2), \tag{12}$$

and from the fourth equation, we have

$$R = \frac{1}{\mu_R}((1-\rho_1) r_1 L_1 + (1-\rho_2) r_2 L_2). \tag{13}$$

We replace Equations (12) and (13) in the first and second equations of system (11), then we will get

$$\begin{cases} L_2 = -\frac{L_1}{\alpha_2}(\alpha_1 - c_1 L_1) = f_1(L_1), \\ L_1 = -\frac{L_2}{\gamma_1}(\gamma_2 - c_2 L_2) = f_2(L_2), \end{cases} \tag{14}$$

with

$$\alpha_1 := \frac{\lambda_1 M_2 \rho_1 r_1}{\mu_V + \delta} + \frac{\lambda_2 K_2 (1-\rho_1) r_1}{\mu_R} - r_1 - \mu_{L_1} = (R_0^1 - 1)\left(r_1 + \mu_{L_1}\right),$$
$$\gamma_2 := \frac{\beta_1 M_1 \rho_2 r_2}{\mu_V + \delta} + \frac{\beta_2 K_1 (1-\rho_2) r_2}{\mu_R} - r_2 - \mu_{L_2} = (R_0^2 - 1)\left(r_2 + \mu_{L_2}\right).$$

We show a unique interior equilibrium exists when these two curves intersect in the interior of the first quadrant. We distinguish several cases depending on the signs of α_1 and γ_2 (see figures). Note that α_1 and γ_2 are, respectively, of the same sign as $(R_0^1 - 1)$ and $(R_0^2 - 1)$.

- (I) $R_0^1 > 1$, $R_0^2 > 1$, In Figure 3, we see that we have one interior equilibrium.
- (II) $R_0^1 > 1$, $R_0^2 < 1$.

In Figure 4, we see that we have one interior equilibrium.

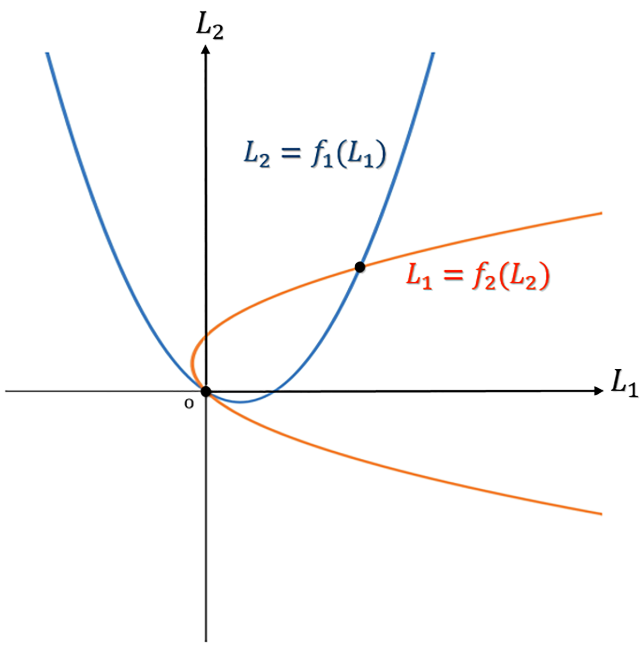

FIGURE 3 Graph of the functions f_1, f_2 for case (I). [Colour figure can be viewed at wileyonlinelibrary.com]

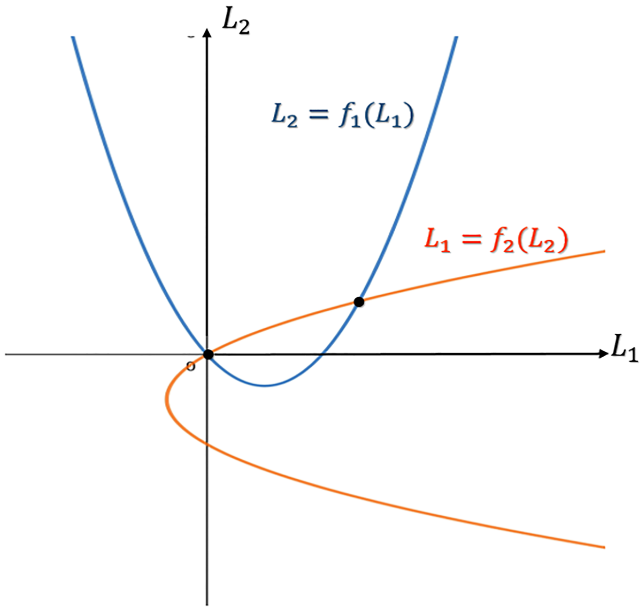

FIGURE 4 Graph of the functions f_1, f_2 for case (II). [Colour figure can be viewed at wileyonlinelibrary.com]

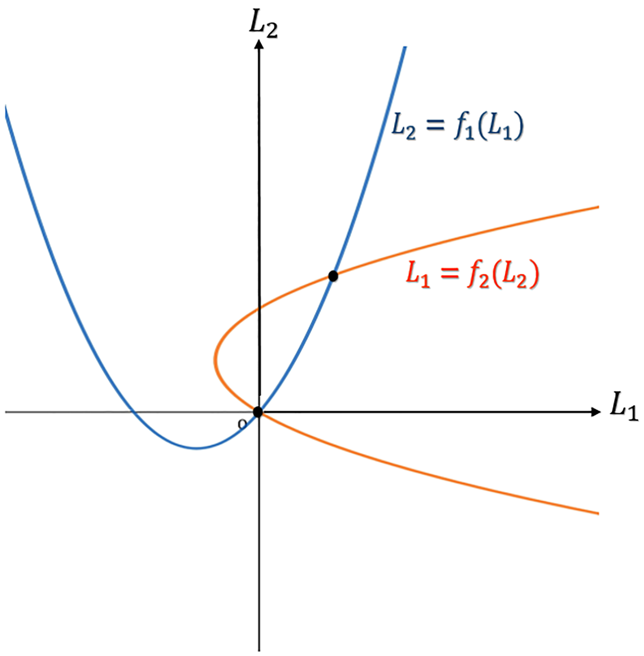

FIGURE 5 Graph of the functions f_1, f_2 for case (III). [Colour figure can be viewed at wileyonlinelibrary.com]

- (III) $R_0^1 < 1$, $R_0^2 > 1$ (Figure 5).
- (IV) $R_0^1 < 1$, $R_0^2 < 1$.

Depending on the signs of the slopes at the origin of the two curves, we distinguish two cases.

$$(a)\ \left.\frac{dL_2}{dL_1}\right|_{L_1=0} = -\frac{\alpha_1}{\alpha_2} > 0, \left.\frac{dL_1}{dL_2}\right|_{L_2=0} = -\frac{\gamma_2}{\gamma_1} > 0,$$

with

$$\left.\frac{dL_2}{dL_1}\right|_{L_1=0} \geq \frac{1}{\left[\frac{dL_1}{dL_2}\right]_{L_2=0}}.$$

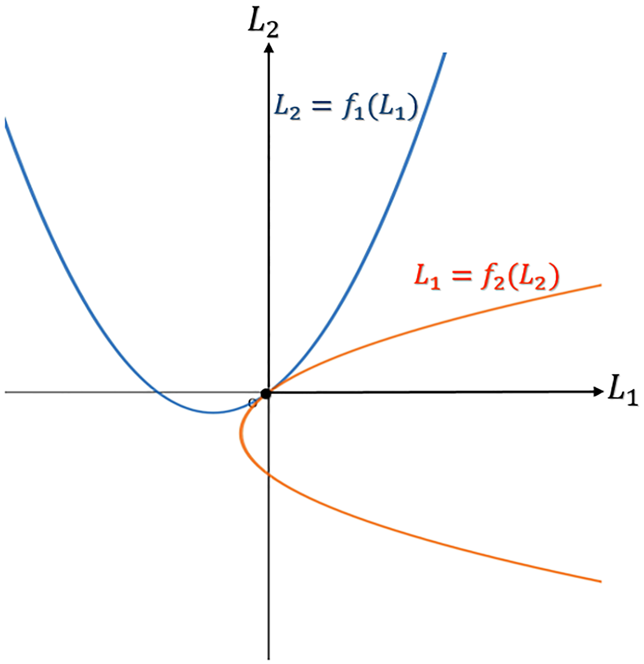

FIGURE 6 Graph of the functions f_1, f_2 for case (IV, a). [Colour figure can be viewed at wileyonlinelibrary.com]

In Figure 6, we see that the curve corresponding to f_2 lies below the curve corresponding to f_1 in the first orthant.

$$(b)\ \left.\frac{dL_2}{dL_1}\right|_{L_1=0} = -\frac{\alpha_1}{\alpha_2} > 0,\ \left.\frac{dL_1}{dL_2}\right|_{L_2=0} = -\frac{\gamma_2}{\gamma_1} > 0,$$

with

$$\left.\frac{dL_2}{dL_1}\right|_{L_1=0} < \frac{1}{\left[\frac{dL_1}{dL_2}\right]_{L_2=0}}.$$

In Figure 7, we see that the curve of f_1 lies below the curve f_2 near the origin in the first orthant.
We summarize the different cases of existence of a positive equilibrium in terms of R_0^i, $i = 1, 2$ in the following diagram:

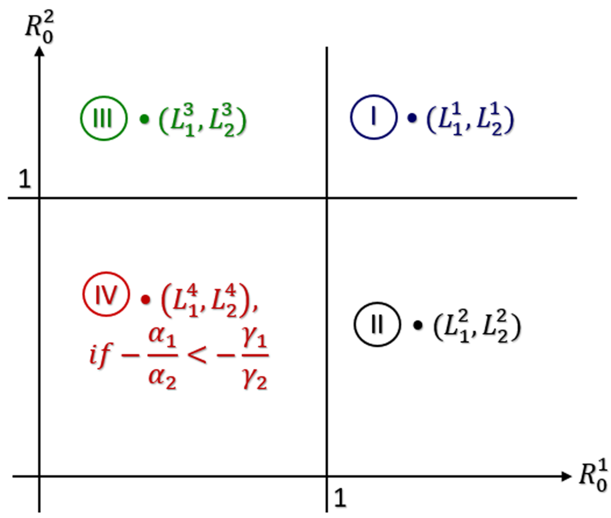

Different zones of existence of positive equilibrium.

In case (IV), the condition

$$-\frac{\alpha_1}{\alpha_2} = -\frac{\gamma_1}{\gamma_2}$$

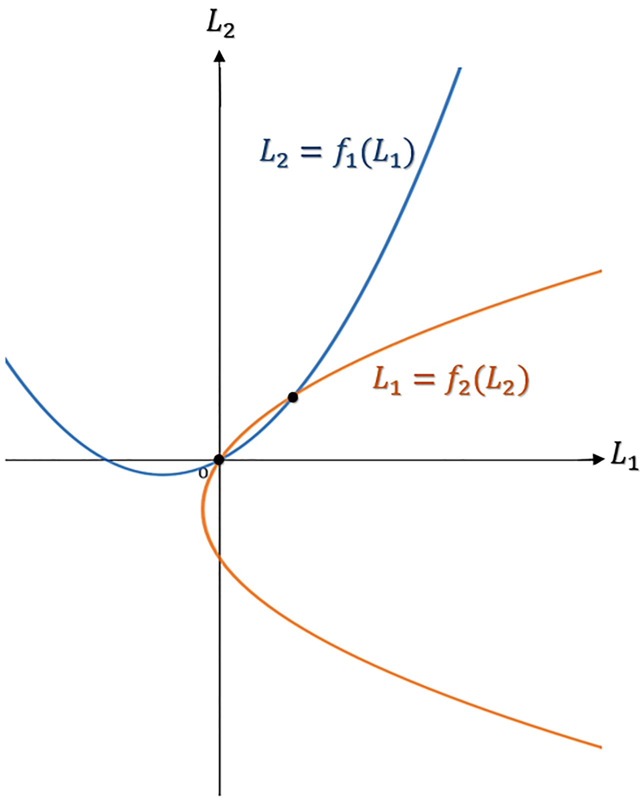

FIGURE 7 Graph of the functions f_1, f_2 for case (IV, b). [Colour figure can be viewed at wileyonlinelibrary.com]

defines in the region $(R_0^1 < 1, R_0^2 < 1)$ a threshold value R_{cri}, with

$$R_{cri} := R_0^2 - \frac{A}{R_0^1 - 1}.$$

Here, A is defined as above, that is,

$$A = \frac{\alpha_2 \gamma_1}{(r_1 + \mu_{L_1})(r_2 + \mu_{L_2})}.$$

Remark 1.

(a) In the region $R_0^i < 1, i = 1, 2$, simple calculations show that $R_{cri} = 1$ if and only if $R_0 = 1$. Similarly, $R_{cri} < 1$ if and only if $R_0 < 1$.
(b) Note that if $A \geq 1$, then $R_{cri} \geq 1$ is always satisfied in the region $R_0^i < 1, i = 1, 2$. However, a necessary condition for $R_{cri} < 1$ to be satisfied is $A < 1$.

We deduce the following existence result.

Proposition 6.

(a) If

$$min(R_0^1, R_0^2) > 1, \tag{15}$$

then system (14) admits a positive equilibrium.

(b) If

$$min(R_0^1, R_0^2) < 1, \ \ and \ \ max(R_0^1, R_0^2) > 1, \tag{16}$$

then system (14) admits a positive equilibrium.

(c) If

$$max(R_0^1, R_0^2) < 1, \ \ and \ \ R_{cri} > 1, \tag{17}$$

then system (14) admits a positive equilibrium.

(d) If

$$max(R_0^1, R_0^2, R_{cri}) < 1, \tag{18}$$

then system (14) admits only the trivial equilibrium.

3.3 | Asymptotic behavior and stability

An essential point of the system (11) is formulated in the following proposition.

Proposition 7.

1. *The trivial equilibrium of system (11) is globally asymptotically stable if*

$$max(R_0^1, R_0^2, R_{cri}) < 1. \tag{19}$$

2. *In case (I), the positive interior equilibrium of system (11) is globally asymptotically stable in $\mathbb{R}_+^4 - \{(L_1, L_2, V, R) : L_1 = L_2 = 0\}$.*

Proof.

1. Let $a = (0, 0, 0, 0)$, then $f(a) \geqslant 0$. Let $L_1^m = L_2^m = m$ be a positive number, large enough such that

$$\lambda_1 M_1 \left(\frac{\rho_1 r_1 + \rho_2 r_2}{\mu_V + \delta} \right) + \lambda_2 K_1 \left(\frac{(1 - \rho_1) r_1 + (1 - \rho_2) r_2}{\mu_R} \right) - r_1 - \mu_{L_1} - c_1 L_1^m < 0,$$

and

$$\beta_1 M_2 \left(\frac{\rho_1 r_1 + \rho_2 r_2}{\mu_V + \delta} \right) + \beta_2 K_2 \left(\frac{(1 - \rho_1) r_1 + (1 - \rho_2) r_2}{\mu_R} \right) - r_2 - \mu_{L_2} - c_2 L_2^m < 0.$$

Let

$$V_m = \frac{\rho_1 r_1 L_1^m + \rho_2 r_2 L_2^m}{\mu_V + \delta},$$

and

$$R_m = \frac{(1 - \rho_1) r_1 L_1^m + (1 - \rho_2) r_2 L_2^m}{\mu_R}.$$

Then, it is clear that $f(b^m) \leqslant 0$ with $b_m = (L_m^1, L_m^2, V_m, R_m)$. Under condition (19), $(0, 0, 0, 0)$ is the unique equilibrium in $[a, b^m]$, then $(0, 0, 0, 0)$ is globally asymptotically stable in $[a, b^m]$, and since b^m can be selected larger than any $x \in \mathbb{R}_+^4$, it follows that $(0, 0, 0, 0)$ is globally asymptotically stable in $\mathbb{R}_+^4$.

2. Let $L_\epsilon^1 = \epsilon > 0$ be small enough such

$$\lambda_1 M_2 \left(\frac{\rho_1 r_1 + \rho_2 r_2}{\mu_V + \delta} \right) + \lambda_2 K_2 \left(\frac{(1 - \rho_1) r_1 + (1 - \rho_2) r_2}{\mu_R} \right) - r_1 - \mu_{L_1} - \epsilon c_1 > 0,$$

since $R_0^1 > 1$. Let $L_\epsilon^2 = \epsilon$ be small enough such

$$\beta_1 M_2 \left(\frac{\rho_1 r_1 + \rho_2 r_2}{\mu_V + \delta} \right) + \beta_2 K_2 \left(\frac{(1 - \rho_1) r_1 + (1 - \rho_2) r_2}{\mu_R} \right) - r_2 - \mu_{L_2} - \epsilon c_2 < 0,$$

since $R_0^2 > 1$. Let

$$V_\epsilon = \epsilon \frac{\rho_1 r_1 + \rho_2 r_2}{\mu_V + \delta}, 0 < \rho_1 < 1,$$

and

$$R_\epsilon = \epsilon\frac{(1-\rho_1)r_1 + (1-\rho_2)r_2}{\mu_R}, 0 < \rho_2 < 1.$$

Then,

$$f(a_\epsilon) \geqslant 0, \ \ with \ \ a_\epsilon = (L_\epsilon^1, L_\epsilon^2, V_\epsilon, R_\epsilon).$$

Under condition $min(R_0^1, R_0^2) > 1$, our system (11) has a unique positive equilibrium point in $[a_\epsilon, b_m]$, since a_ϵ can be selected arbitrarily small, and b_m larger than any $x \in \mathbb{R}_+^4$, then the interior positive equilibrium is globally asymptotically stable in interior of $\mathbb{R}_+^4$. When $L_1 = L_2 = 0$, the equations of V and R are decreasing and converges to zero. □

Remark 2.

1. If the two patches do not sustain the population $max(R_0^1, R_0^2) < 1$, then under condition $R_{cri} < 1$, the metapopulation will not survive. In the case, when all individuals (adults and juveniles) are able to move between patches, the authors in Marva and San Seguendo [17] show that under suitable conditions two viable populations leads to extinction when they are linked.
2. If the population is able to survive in every patch, $min(R_0^1, R_0^2) > 1$, then the population will persist in the entire system. In this case, the model shows realistic behavior and dispersal cannot affect the survival.
3. There are a number of questions remaining for future studies. For example, the global stability of the positive equilibrium in cases (*II*), (*III*), and (*IV*). We limit ourselves to numerical simulations. In Figure 6, we show that when an unfavorable patch ($R_0^1 < 1$) is connected to another unfavorable patch ($R_0^2 < 1$), the metapopulation can go to extinction despite the existence of a positive equilibrium. In the case when all individuals (adults and juveniles) move between patches, we mention the interesting results obtained in Marva and San Seguendo [17], where the authors showed that there is a setting enabling a metapopulation of two connected sink patches ($R_0^i < 1, i = 1, 2$) to survive. Figure 5 illustrates the case of an unfavorable patch ($R_0^1 < 1$) connected to a favorable patch ($R_0^2 > 1$), the model predict that the total population will survive.

3.4 | Numerical simulations

In this section, we use numerical simulations to confirm theoretical results. Figures 8–13 illustrate the fact that systems (7) and (11) produce similar behaviors when ϵ is small enough. If $R_0^i > 1, i = 1, 2$, both systems evolve to a positive equilibrium. If $R_0^i \leq 1, i = 1, 2$ and $R_{cri} < 1$, both systems go to the trivial equilibrium. The reduced system (11) provides a good approximation of the dynamic behavior of the initial system (7) when ϵ is small enough.

The values of parameters used for Figures 8–10 are as follows:

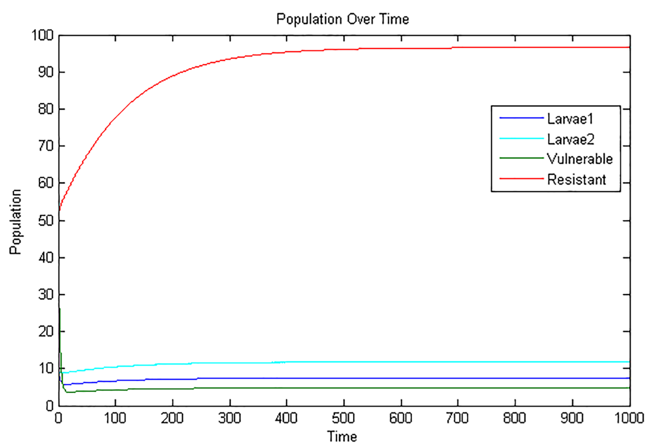

FIGURE 8 The behavior of system (11) trajectories for a reproduction rate $R_0^i > 1, i = 1, 2$. [Colour figure can be viewed at wileyonlinelibrary.com]

λ_1	λ_2	r_1	r_2	μ_{L_1}	μ_{L_2}	c_1	c_2	μ_{V_1}	μ_{V_2}	μ_{R_1}
0.5	0.4	0.2	0.2	0.2	0.2	0.2	0.2	0.2	0.2	0.02
μ_{R_2}	ρ_1	ρ_2	δ_1	δ_2	β_1	β_2	m^1	m^2	k^1	k^2
0.02	0.5	0.5	0.2	0.2	0.4	0.5	0.01	0.02	0.02	0.01

The values of parameters used for Figures 11–13 are as follows:

λ_1	λ_2	r_1	r_2	μ_{L_1}	μ_{L_2}	c_1	c_2	μ_{V_1}	μ_{V_2}	μ_{R_1}
0.5	0.4	0.2	0.2	0.2	0.2	0.2	0.2	0.2	0.2	0.2
μ_{R_2}	ρ_1	ρ_2	δ_1	δ_2	β_1	β_2	m^1	m^2	k^1	k^2
0.2	0.5	0.5	0.2	0.2	0.4	0.5	0.01	0.02	0.02	0.01

The basic reference of measurement of parameters is 1 day = d = unit of slow time τ, which corresponds to unit of fast time $t = \frac{d}{\epsilon}$. The dispersal parameters are measured per 1 s. A close look at these parameters show that for example $m^1 = 0.01/\text{s} = 14.4/\text{day}$ and $\lambda_1 = 0.5/\text{day}$. This means that dispersal parameters are much larger than demographic parameters.

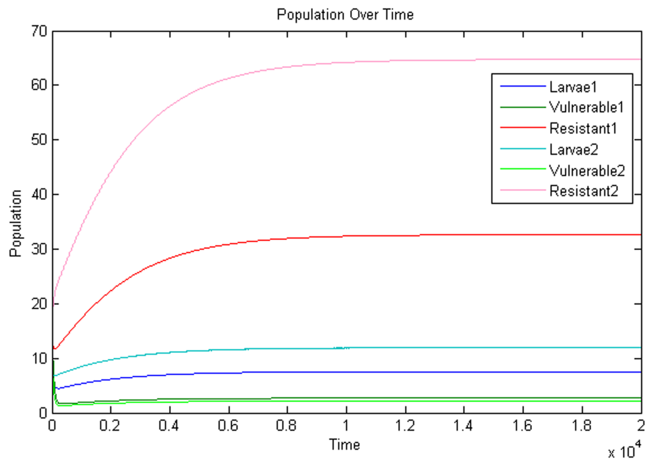

FIGURE 9 The behavior of system (7) trajectories for a reproduction rate $R_0^i > 1, i = 1, 2$, and for $\epsilon = 0.05$. [Colour figure can be viewed at wileyonlinelibrary.com]

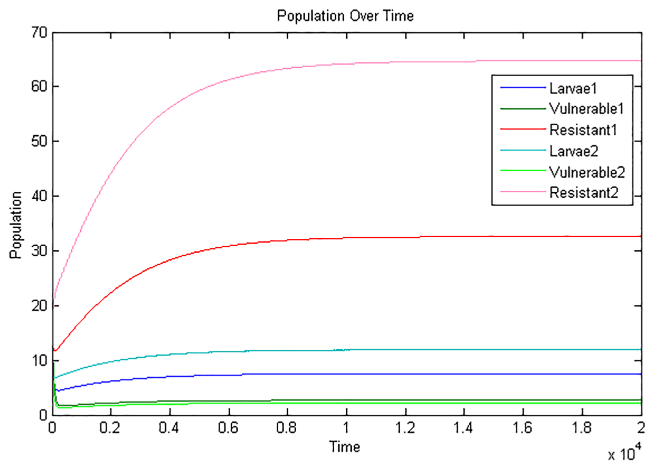

FIGURE 10 The behavior of system (7) trajectories for a reproduction rate $R_0^i > 1, i = 1, 2$, and for $\epsilon = 0.01$. [Colour figure can be viewed at wileyonlinelibrary.com]

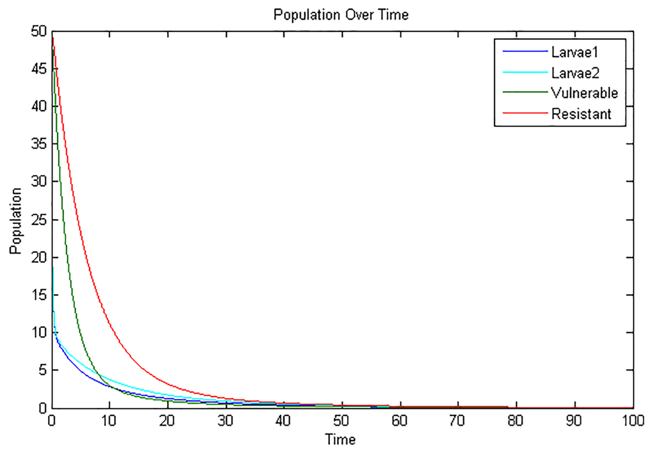

FIGURE 11 The behavior of system (11) trajectories for a reproduction rate $R_0^i < 1$, $i = 1, 2$, $R_{cri} < 1$. [Colour figure can be viewed at wileyonlinelibrary.com]

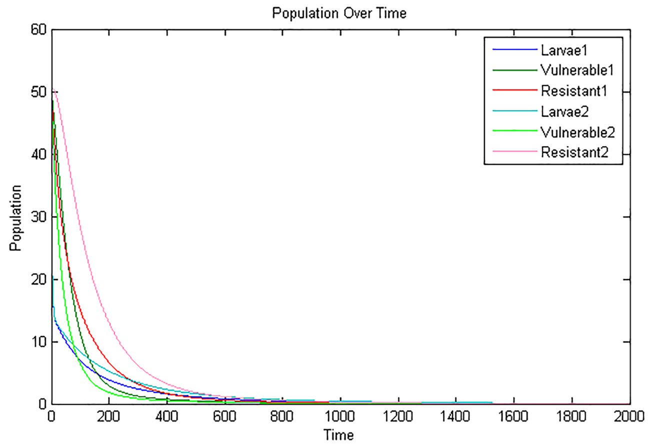

FIGURE 12 The behavior of system (7) for a reproduction rate $R_0^i < 1, i = 1, 2$, $R_{cri} < 1$, and $\epsilon = 0.05$. [Colour figure can be viewed at wileyonlinelibrary.com]

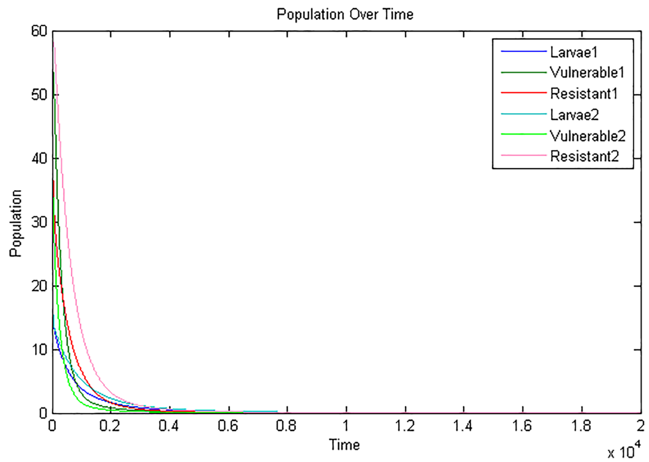

FIGURE 13 The behavior of system (7) for a reproduction rate $R_0^i < 1, i = 1, 2$, $R_{cri} < 1$, and $\epsilon = 0.01$. [Colour figure can be viewed at wileyonlinelibrary.com]

In Figure 14, we see that a pest favorable patch can maintain the pest population in the unfavorable patch, and in Figure 15, we see that if the two patches are defavorable to the pest, then the behavior of the global system (11) can also be defavorable even if $R_{cri} > 1$.

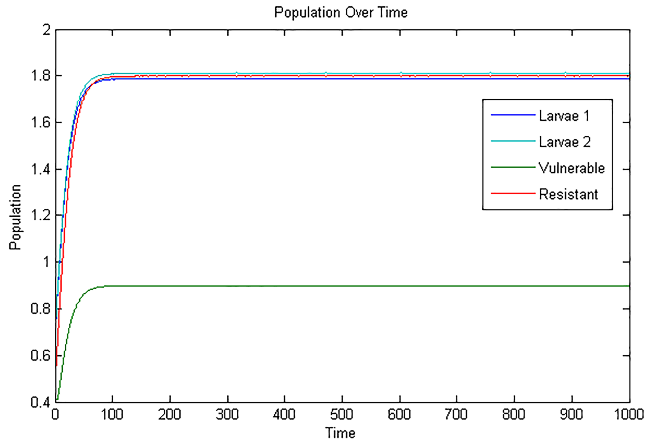

FIGURE 14 The behavior of system (11) trajectories for a reproduction rate $R_0^1 < 1, R_0^2 > 1$, $\lambda_1 = 0.76$, $\lambda_2 = 0.76$, $r_1 = 0.2$, $r_2 = 0.2$, $\mu_{L_1} = 0.2$, $\mu_{L_2} = 0.2$, $c_1 = 0.2$, $c_2 = 0.2$, $\mu_{V_1} = 0.2$, $\mu_{V_2} = 0.2$, $\mu_{R_1} = 0.2$, $\mu_{R_2} = 0.2\rho_1 = 0.5$, $\rho_2 = 0.5$, $\delta_1 = 0.2$, $\delta_2 = 0.2$, $\beta_1 = 1.55$, $\beta_2 = 1.55$, $m^1 = 0.01$, $m^2 = 0.02$, $k^1 = 0.01$, $k^2 = 0.02$. [Colour figure can be viewed at wileyonlinelibrary.com]

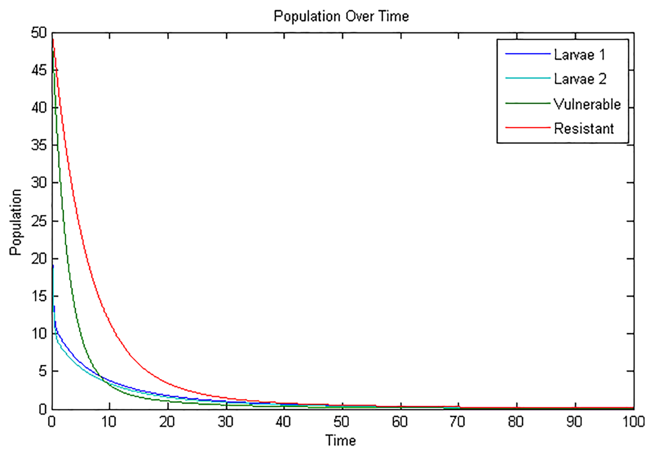

FIGURE 15 The behavior of system (11) trajectories for a reproduction rate $R_0^1 < 1, R_0^2 < 1$, $R_{cri} > 1$, $\lambda_1 = 0.5$, $\lambda_2 = 0.4$, $r_1 = 0.2$, $r_2 = 0.2$, $\mu_{L_1} = 0.2$, $\mu_{L_2} = 0.2$, $c_1 = 0.2$, $c_2 = 0.2$, $\mu_{V_1} = 0.2$, $\mu_{V_2} = 0.2$, $\mu_{R_1} = 0.2$, $\mu_{R_2} = 0.2$, $\rho_1 = 0.5$, $\rho_2 = 0.5$, $\delta_1 = 0.2$, $\delta_2 = 0.2$, $\beta_1 = 0.7$, $\beta_2 = 0.7$, $m^1 = 0.01$, $m^2 = 0.02$, $k^1 = 0.01$, $k^2 = 0.02$. [Colour figure can be viewed at wileyonlinelibrary.com]

4 | CONCLUDING REMARKS

The model we have studied in this paper can be applied to other pests with the same characteristics. We have studied the nonlinear dynamics of a three dimensional differential system describing the evolution of a vineyard pest population called *L. botrana*. We have established the well-posedness of the system. The model has two equilibriums, and we have determined a sharp threshold R_0 whose value determines whether the pest population goes to extinction or persists. Under suitable conditions, the proposed model undergoes a transcritical bifurcation. Although some parameters are difficult to obtain, like the proportion of new resistant insects or the insect mortality induced by insecticides, numerical simulations are provided and agree well with the theoretical results. Additional measures will be needed to control the pest population. A combination of sexual confusion technique and insecticides could be efficient for controlling the pest population. Note that the technique of sexual confusion makes the males of the species unable to find the true female.

Similarly to Thiéry et al. [9], we show that the larvae crowding do not alter the reproduction capacity of the pest. This is explained by the fact that R_0 does not depend on the juvenile competition rate c. It follows from the formula of R_0 that in the case of an intensive treatment by insecticides, and a low rate of mutation, the rapid evolution towards resistance (λ_2 is large enough) leads to a dramatic situation. In the second part of the paper, we considered a patchy model. We restricted our attention to the case where the number of patches $N = 2$. Using aggregation method based on the existence of different time scales, we formulated a reduced model with a small number of variables. The study shows that population dynamics are highly dependent on local patch conditions and the nature of the movement between patches. Of course, the case of several patches is more general and realistic. However, it is difficult to make similar mathematical analysis, and the question is open. In Remark 1 (b), it is shown that the condition $A < 1$ contributes to reduce the population of insects. This condition is obtained, for instance, if the movement is asymmetric. More precisely, either m_1, k_1 are small enough and the movement towards Patch 1 is more important or m_2, k_2 are small enough and the movement towards Patch 2 is more important. This finding agrees with the results obtained in Vuilleumier and Possingham [18]. In the same context, we refer the readers to Marva and San Seguendo [17], where the authors show with an age-structured model that changes in the strategy of the movement between patches may drastically change the long-term behavior of the whole metapopulation.

A possible scenario corresponding to Figure 5 is the theoretical example when Patch 1 is treated ($\delta > 0$) containing mostly vulnerable adults, connected to untreated Patch 2 ($\delta = 0$), containing mostly resistant adults. When the population of Patch 1 emigrates to Patch 2, and conversely that of Patch 2 emigrates to Patch 1, the total population of the system will survive. On this type of questions, we refer the reader to Helps et al. [19].

In our model, there is no competition among adults for hosts and mates [10], but this could be possible for other insect models. Figure 6 shows that threshold existence of positive equilibrium does not necessarily coincide with survival threshold. The basic reproduction number R_0 is a function of eight parameters; see Section 2.3. There are several methods to calculate the basic offspring number, including survival function, the graph theoretic method, and the next generation method. We refer the reader to Heffernan et al. [20] for a summary of these methods. Local sensitivity analysis of the basic reproduction number R_0 with respect to a parameter can be done using the partial derivative of R_0 with respect to its arguments, see Caribon et al. [21], it could be performed to determine parameters with higher influence on the insect pest dynamic. This will be the scope of a future work. Note that diapauses is a strategic mechanism for insects to avoid adverse environmental conditions which is not considered in this paper. It would be interesting to consider the possibility that the pest can undergo a diapause at the pupae stage which would lead to differential equations with delays. Some results are in preparation in this direction.

ACKNOWLEDGEMENTS

The authors are grateful to the anonymous referees, who provided valuable suggestions and insight that greatly improved the paper.

CONFLICT OF INTEREST STATEMENT

This work does not have any conflicts of interest.

ORCID

Ainseba Bedreddine https://orcid.org/0000-0001-6449-428X
Bouguima Sidi Mohammed https://orcid.org/0000-0001-8626-6405

REFERENCES

1. F. Pavan, G. Bigot, E. Cargnus, and P. Zandigiacomo, *Influence of the carpophagous generations of the European grapevine moth Lobesia botrana on grape bunch rots*, Phytoparasiticia **42** (2014), 61–69.
2. N. Maher and D. Thiéry, *Daphne gnidium, a possible native host plant of the European grapevine moth Lobesia botrana, stimulates its oviposition. Is a host shift relevant?* Chemoecology **16** (2006), 135–144.
3. R. Levins, *Some demographic and genetic consequences of environmental heterogeneity for biological control*, Bull. Entomol. Soc Am. **15** (1969), 237–240.
4. F. J. Irigaray, V. Marco, F. G. Zalom, and I. P. Moreno, *Effects of methoxyfenozide on Lobesia botrana (Lepidoptera: Tortricidae) egg, larval and adult stages*, Pest. Manag. Sci. **2005** (2005), 61–11.
5. J. Hemingway, J. Field, and J. Vontas, *An overview of insecticide resistance*, Science **298** (2002), 96–97.
6. B. Ainseba, D. Picart, and D. Thiéry, *An innovative multistage, physiologically structured population model to understand the European grapevine moth dynamics*, J. Math. Anal. Appl. **382** (2011), 34–46.
7. D. Picart and F. Milner, *Optimal control in a multistage physiologically structured insect population model*, Appl. Math. Comput. **247** (2014), 973–588.
8. Y. He. (2013). *Analyse et contrôle de modèles de dynamique de populations*, PhD Thesis, Université Bordeaux 1, Bordeaux.

9. D. Thiéry, K. Monceau, and J. Moreau, *Larval intraspecific competition for food in the European grape vine moth Lobesia botrana*, Bull. Entomol. Res. **104** (2014), no. N4, 517–524.
10. D. Picart. (2009). *Modélisation et Estimation des Paramètres Li és au Succès Reproducteur d'un Ravageur de la Vigne (Lobésia Botrana)*, PhD Thesis, Bordeaux I University, Bordeaux.
11. C. D. Meyer, *Matrix Analysis and Applied Linear Algebra*, Har/Cdr, SIAM, Philadelphia, 2000.
12. P. van den Driessche and J. Watmough, *Reproduction numbers and sub-threshold endemic equilibria for compartmental models of disease transmission*, Math. Biosci. **180** (2002), 1–2.
13. R. Anguelov, Y. Dumont, and J. Lubuma, *Mathematical modelling of sterile insect technology for control of anopheles mosquito*, Comput. Math. Appl. **64** (2012), 374–389.
14. J. C. Poggiale. (1994). *Application des variétés invariants à la modélisation de l'hétérogénieté en dynamique des populations*, PhD Thesis, Université Dijon, Dijon.
15. P. Auger and R. Bravo de la Parra, *Methods of aggregation of variables in population dynamics*, C. R. Acad. Sci. Paris, Sci. de la Vie. **323** (2000), 665–674.
16. A. Harrak, A. Bergam, T. Nguyen-Huu, P. Auger, and R. Mchich, *Application of aggregation of variables methods to a class of two-time reaction-diffusion-chemotaxis models of spatially structured populations with constant diffusion*, Discret. Contin. Dyn. Syst. B. **14** (2021), no. 7, 2163–2181.
17. M. Marva and F. San Seguendo, *Age structure density-dependent fertility and individuals dispersal in population models*, Math. Biosci. **300** (2018), 157–167.
18. S. Vuilleumier and H. P. Possingham, *Does colonization asymmetry in metapopulation*, Proc. R. Soc. B. **273** (2006), 1637–1642.
19. J. C. Helps, N. D. Paveley, and F. Vander Bosh, *Identifying circumstances under which high insecticide dose increases or decreases resistance selection*, J. Theor. Biol. **428** (2017), 153–167.
20. J. M. Heffernan, R. J. Smith, and L. M. Wahl, *Perspectives on the basic reproduction ratio*, J. Royal Soc. Interface **2** (2005), no. 4, 281–293.
21. J. Caribon, D. Gatelli, R. Liska, and A. Saltelli, *The role of sensitivity analysis in ecological modelling*, Ecol. Model. **203** (2007), no. 1-2, 167.
22. S. Cirolani, M. Boselli, A. Butturini, M. Chicca, E. A. Fano, and S. Cassanelli, *Assessment of insecticide resistance of Lobesia botrana (Lepidoptea:Tortricidae) in Emilia-Romagna region*, J. Econ. Entomol. **107** (2014), 1245–1249.
23. H. R. Smith and MD Systems, *Monotone Dynamical Systems*, Mathematical Survey and Monographs, Vol. **41**, AMS, Providence, Rhode Island, 1995.

How to cite this article: K. Khadidja Aicha, A. Bedreddine, and B. Sidi Mohammed, *Mathematical modeling of pest resistance to insecticides in a heterogeneous environment*, Math. Meth. Appl. Sci. **46** (2023), 13320–13341. DOI10.1002/mma.9254